Preparation and Characterization of PSt-*b*-PHEMA Metal Hybrids

YANMEI WANG,[1] JINGSHEN WU,[2] JINYING YUAN,[3] GUIFEN SUN,[4] CAIYUAN PAN[1]

[1] Department of Polymer Science and Engineering, University of Science and Technology of China, Hefei, 230026, People's Republic of China

[2] Department of Mechanical Engineering, Hong Kong University of Science and Technology, Kowloon, Hong Kong, People's Republic of China

[3] Department of Polymer Science and Engineering, Beijing University, Beijing, 100871, People's Republic of China

[4] EM Lab of Changchun Institute of Applied Chemistry, Chinese Academy of Science, Changchun, 130022, People's Republic of China

ABSTRACT: The block copolymer polystyrene-*b*-poly[2-(trimethylsilyloxy)ethylene methacrylate] (PSt-*b*-PTMSEMA) was synthesized using atom-transfer radical polymerization (ATRP). The hydrolysis of PSt-*b*-PTMSEMA led to the formation of an amphiphilic block copolymer, polystyrene-*b*-poly(2-hydroxylethyl methacrylate) (PSt-*b*-PHEMA), which was characterized by GPC and ^{1}H-NMR. TEM showed that the PSt-*b*-PHEMA formed a micelle, which is PSt as the core and PHEMA as the shell. Under appropriate conditions, the nickel or cobalt ion cause chemical reactions in these micelles and could be reduced easily. ESCA analysis showed that before reduction the metal existed as a hydroxide; after reduction, the metal existed as an oxide, and the metal content of these materials on the surface is more than that on the surface of the copolymer metal ion. XRD analysis showed that the metal existed as a hydroxide before reduction and existed as a metal after reduction. © 2002 John Wiley & Sons, Inc. J Appl Polym Sci 83: 2883–2891, 2002; DOI 10.1002/app.10278

Key words: atomic-transfer radical polymerization (ATRP); block copolymers; block copolymer metal hybrids

INTRODUCTION

Hybridization of polymer gels and metal nanoclusters is very beneficial and interesting in the development of polymer conductors, optical materials, and catalyst carriers.[1] To control the functionality of these composite materials, the location of metal nanoclusters in the gels should be controlled. For this reason, the microphase-separated structures of amphiphilic block copolymers were used as templates. An alternative application of amphiphilic block copolymers is the exploitation of their stable micelles as "molecular reaction flasks"; in such micelles, chemical and physical reactions can be confined to the fluid micellear cores, the size of which are measured on a nanometer scale.[2–4] This possibility is especially relevant with respect to a reaction that afford solids, such as reductions or precipitation of oxides and sulfides, as the size of the product is

Table I   Preparation and Characterization of PSt and PSt-*b*-PHEMA

Sample[a]	[M] : [I][b] (mol ratio)	M_n (GPC)	M_n (NMR)	$n : m$[c]	M_w/M_n[d]	Core (nm)	Corona (nm)
A	200 : 1	12190	12400	117 : 0	1.42	60	
B	70 : 1		16500	117 : 21	1.37	20	10

[a] A represents PSt; bulk polymerization, EBB/CuBr/bpy = 1 : 1 : 3 (molar ratio), 110°C, 16 h; B represents block PSt-*b*-PHEMA, bulk polymerization, PSt–Br/CuBr/bpy = 1 : 1 : 3 (molar ratio), 80°C, 12 h.

[b] [M] : [I] means monomer : initiator.

[c] The ratio of the polymerization degree of PSt (*n*) block and PHEMA (*m*) block, calculated based on ^{1}H-NMR data.

[d] For block copolymer, GPC measurement before hydrolysis of the block copolymer.

limited by the mesoscopic reaction flask. Thus, the block copolymer micelles are initially loaded with the reactants, for example, metal salts. Generally, this does not affect the structural parameters of micelles with high interfacial energy. Cohen et al.[5–7] succeeded in introducing several types of metal nanoclusters into the lamella and spherical microdomains in diblock copolymer films. Ishizu et al.[8,9] prepared anisotropically semiconducting films by exposing a poly(styrene-*b*-2-vinylpyridine) diblock copolymer (S2VP) with oriented lamellar and spherical microdomains to alkyl halide vapors. They also introduced colloidal silver into quarternized 2VP lamellae by the reduction of silver iodide.[10] Antonietti et al.[4,11,12] studied the block copolymer of polystyrene-*b*-poly(4)vinylpyridine, which stabilizes a whole range of semiconductor and metal colloids.

For the above purposes, the preparation of an amphiphilic block copolymer is very important. Living polymerizations, mainly performed by anionic, cationic, or group-transfer polymerization, appear to be the best technique to reach this target. However, these living polymerizations require specific experimental conditions that often make their industrial application difficult. Recently, one of the most successful controlled/"living" radical polymerization methods developed is atom-transfer radical polymerization (ATRP).[13] ATRP has been proven to be effective for a wide range of monomers[14] and appears to be a powerful tool for the polymer chemist, providing new possibilities in structural and architectural design[15] and allowing the development of new materials with monomers currently available.

This article investigated the preparation of polystyrene-*b*-poly(2-hydroxylethyl methacrylate) (PSt-*b*-PHEMA) and Ni^{2+}/, Ni (0)/, Co^{2+}/, and Co (0)/PSt-*b*-PHEMA composites. Their microphase-separation behaviors were also studied.

EXPERIMENTAL

Materials

CuBr was washed with acetic acid, followed by methanol to remove impurities. 2,2′-Bipyridine (bpy) was used as received. Ethyl α-bromobutyrate (EBB) was prepared by the reaction of α-bromobutyric acid and ethanol in the presence of *p*-toluene sulfonic acid. Styrene (St; chemical reagent, Central Chemical Plant of Shanghai Chemical Reagent Station, Shanghai, China) was distilled at 40°C/14.5 mmHg and stored at 4°C. 2-Hydroxyethyl methacrylate (HEMA) was purified by initially dissolving the monomer in water (25 vol %) containing hydroquinone (0.1 wt %). The solution was extracted 10 times with hexane to remove diacrylates and the aqueous solution
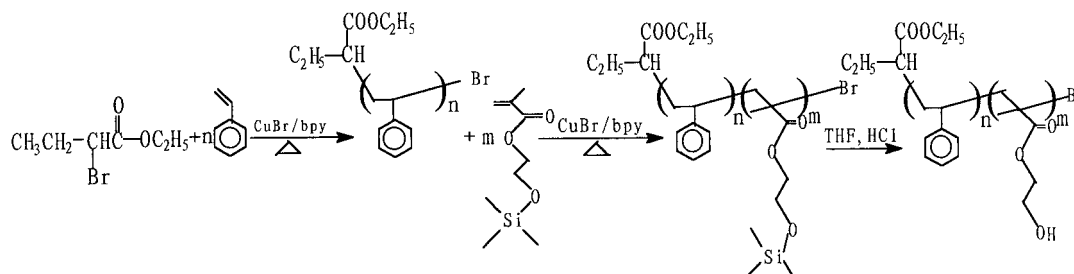
Scheme 1

was salted (200 g of NaCl/L). The monomer was then separated from the aqueous phase by diethyl ether extraction (four times) to remove acrylic acid. Hydroquinone (0.05 wt %) and $MgSO_4$ (3 wt %) were added to the ether solution before the ether was distilled. The purified monomer was distilled at 70°C/2 mmHg immediately prior to use. Nickel chloride hexahydrate ($NiCl_2 \cdot 6H_2O$,), cobalt chloride hexahydrate ($CoCl_2 \cdot 6H_2O$), and KBH_4 were analytical grade and used without further purification.

Preparation of 2-Trimethylsilyloxyethyl Methacrylate (TMSEMA)

TMSEMA was synthesized by silylation of HEMA (26 mL) with trimethylsilyl chloride (41 mL) in CH_2Cl_2/NEt_3 (200/50 mL) at 0°C under N_2 for 2 h and then allowed to come to room temperature. The solution was filtered to remove $NEt_3 \cdot HCl$, and the volatile compounds were removed by distillation. The reaction mixture was filtered again, then dissolved in ethyl acetate (170 mL) and washed with water three times. The organic solution was dried and low boiling point volatiles were evaporated off, and the product was distilled and collected at 63°C/3 mmHg. Yield: 85%.

^{1}H-NMR(CDCl$_3$): δ6.1 (1H); 5.5 (1H); 4.2 (2H); 3.8 (2H); 1.9 (3H); 0. 5(9H).

Preparation of PSt-*b*-PHEMA Copolymer

The polymerizations were conducted in a sealed tube. CuBr, bpy, the monomer(s), and initiator were added to the sealed tube, the mixture was degassed by three freeze–pump–thaw cycles, sealed under N_2, and placed in a preheated oil bath. After a definite time, the mixture was cooled to room temperature rapidly and opened. The reaction mixture was diluted with THF (1:1 to 1:4 v/v) and filtered through a neutral alumina column to remove the catalyst, and the sample was taken for GPC analysis. The rest of the solution was concentrated using a rotating evaporator, and the polymer was dried in vacuum at 60−80°C /0.1 mmHg.

Block copolymerizations were conducted as follows: The homopolymers, isolated as described above, were used as macroinitiators for the polymerization of the second monomer. The feed ratios and conditions are listed in Table I.

The block copolymer, PSt-*b*-PTMSEMA (0.2 g), was dissolved in 5 mL of THF and 0.5 mL of H_2O containing 3 drops of HCl added while magnetically stirring. After 30 min, the slightly yellow
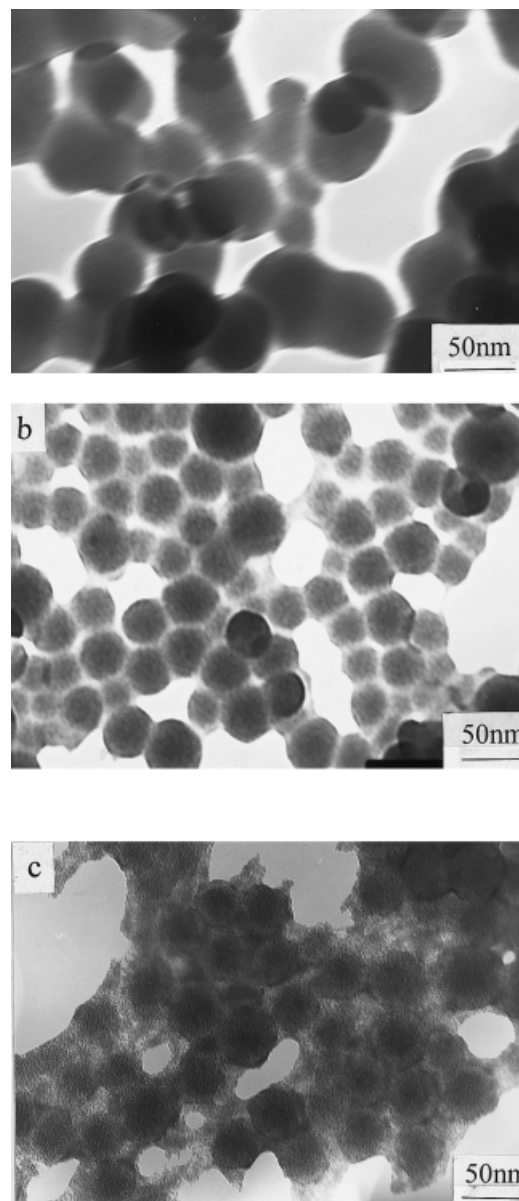

Figure 1 TEM photos of (a) PSt homopolymer, (b) PSt-*b*-PHEMA block copolymer, and (c) PSt-*b*-PHEMA block copolymer stained by RuO$_4$.

solution obtained was added dropwise to 60 mL of H_2O, whereby a fine precipitate was formed. The mixture was neutralized with 5% NaOH and the PSt-*b*-PHEMA copolymer was isolated by centrifugation and dried at 40°C/0.1 mmHg. This procedure is listed in Scheme 1.

Preparation of PSt-*b*-PHEMA Metal Hybrids

The block copolymer (0.2 g) was dissolved in DMF (20 mL) at 70°C, and 1 mL of a $NiCl_2 \cdot 6H_2O$ (0.15 g) ammonia solution (pH 10) was added; then, the
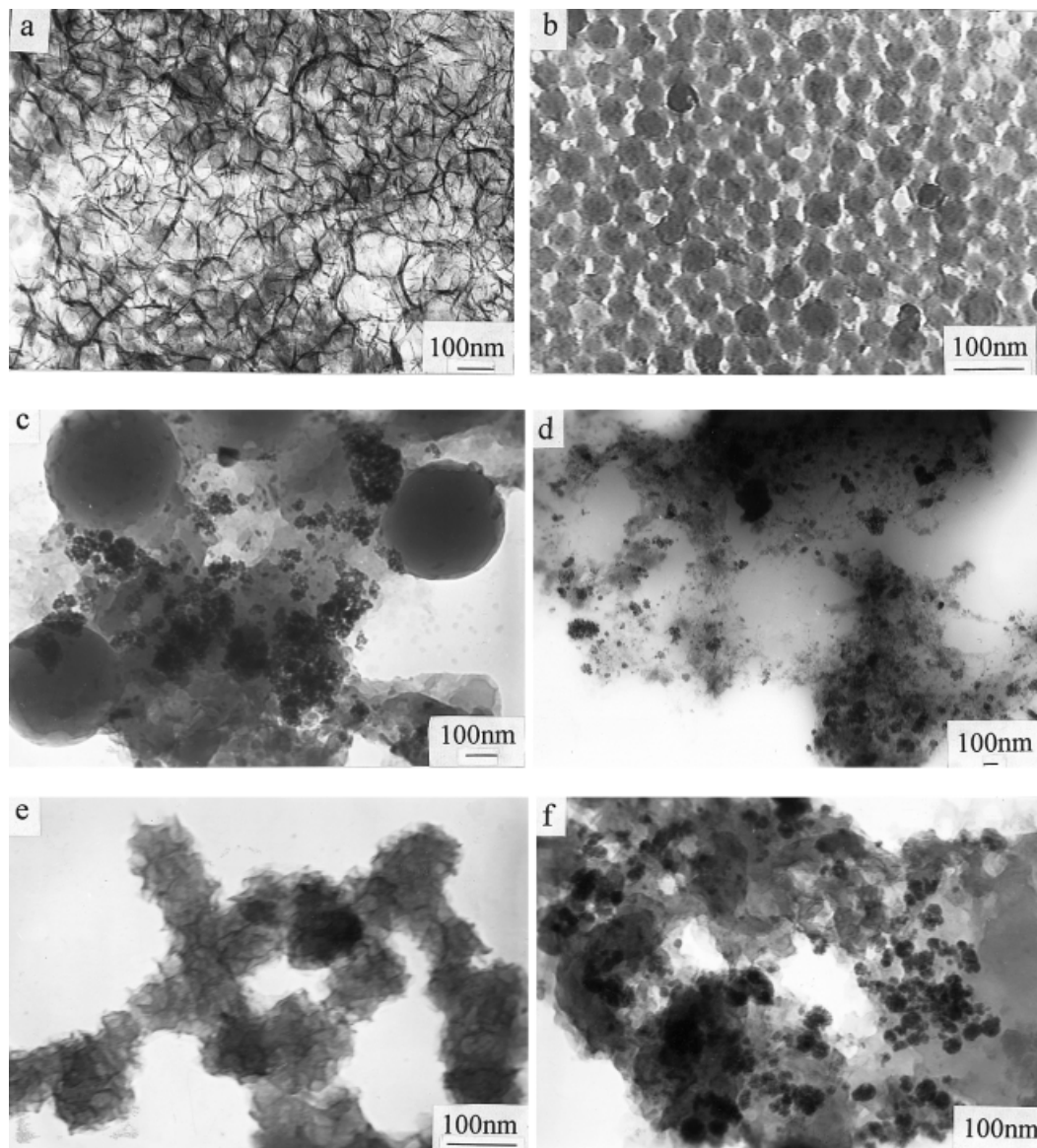
Figure 2 TEM photos of (a) B-1, (b) B-11, (c) B-2, (d) B-22, (e) B-3, and (f) B-33.

solution was stirred at 70°C for 5 h and dispersed in 200 mL H_2O and the dispersion was separated using a filter and redispersed in the water. The above procedure was repeated until the pH value of the filtrate was 7.0. Then, the dispersion was dried at room temperature in a vacuum. A green powder was obtained and dispersed in water. To this dispersion, a KBH_4 (0.15 g) solution in water was added and stirred for 1 h at 45°C, and the mixture was filtered and redispersed in the water. The above procedure was repeated until the pH value of the filtrate was 7.0. Then, the solid was dried at room temperature in a vacuum. A black powder was obtained. The magnetic property of the powders was qualitatively confirmed

using a simple magnetic stirring bar. The procedure of preparing the PSt-*b*-PHEMA cobalt compound is almost the same as that of preparing PSt-*b*-PHEMA nickel. The difference is that the $CoCl_2 \cdot H_2O$ ammonia solution was added into the PSt-*b*-PHEMA solution and then a red powder was formed; after the red powder was reduced by KBH_4, a black powder was formed. The preparation procedure of the PSt-*b*-PHEMA nickel/cobalt alloy is almost the same as the above process. The difference is that the $CoCl_2 \cdot 6H_2O$ (0.15 g) and $NiCl_2 \cdot H_2O$ (0.15 g) ammonia solution was added into the PSt-*b*-PHEMA (0.2 g, 20 mL DMF) solution. A red powder was formed, and when reduced using KBH_4 (0.3 g), a black powder was formed.
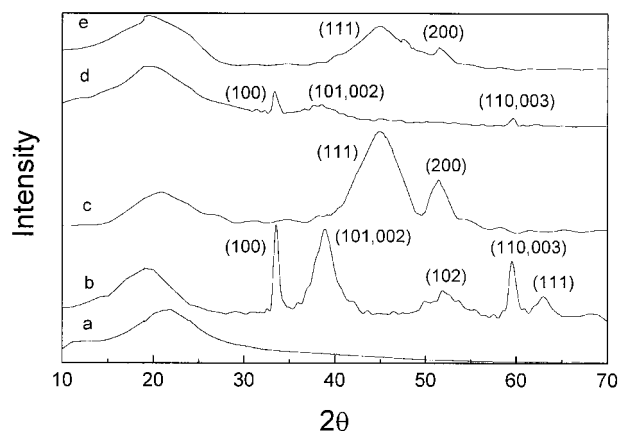
Figure 3 XRD of (a) B, (b) B-1, (c) B-11, (d) B-3, and (e) B-33.

The black PSt-*b*-PHEMA/Co and black PSt-*b*-PHEMA/Ni Co alloy composite particles have a magnetic property.

Characterization

Gel permeation chromatography (GPC) was carried out on a Waters 510 HPLC pump equipped with three polystyrene gels 5×10^5, 5×10^4, and 500 Å columns in series. THF used as the fluent with a Waters 410 differential refractometer and polystyrene as the standard. Measurements of ^{1}H-NMR spectra were performed in a DMX-500 NMR spectrometer. Electron spectroscopy chemical analysis (ESCA) spectra were obtained using an ESCALAB MK-II with an MgKα X-ray source radiation generated at 12 kV and 20 mA. The size and morphology of PSt-*b*-PHEMA and its metal compound were investigated by transmission electron microscopy (TEM, H-800 microscope)

and X-ray diffraction (XRD, D/max-rA). The PSt or PSt-*b*-PHEMA was dissolved in DMF (1 wt %). A drop of the sample was cast onto a copper microgrid coated with carbon. The polymer solution was dried gradually at room temperature. The specimen was dried another 8 h at 70°C. The morphology of the microphase separation was observed with a transmission electron microscope. The nickel and cobalt contents in the PSt-*b*-PHEMA metal compound were measured by an atomic absorption spectrum (Atomscan Advantage, Thermo Jarrell Ash Corp., USA).

RESULTS AND DISCUSSION

Characterization of Copolymer

The molecular weight of the homopolymer PSt obtained from GPC or ^{1}H-NMR was almost the same. The number-average degrees of polymerization of PSt (n) and PHEMA (m) were determined by ^{1}H-NMR, and the polydispersity indices (M_w/M_n) were determined by GPC using polystyrene as a calibration standard. Polymers with low polydispersities ($M_w/M_n < 1.5$) were obtained by ATRP (Table I).

The morphologies of the homopolymer PSt (A) and the block copolymer PSt-*b*-PHEMA (B) were examined by TEM and are shown in Figure 1, and found when comparing Figure 1(a) with Figure 1(b) and 1(c), they were found to be completely different The block copolymer shows a core–shell-type micelle. Since ruthenium tetraoxide (RuO$_4$) is expected to react with double bonds, the dark parts in the photographs thus correspond to PSt, which formed a spherical core of the particle with
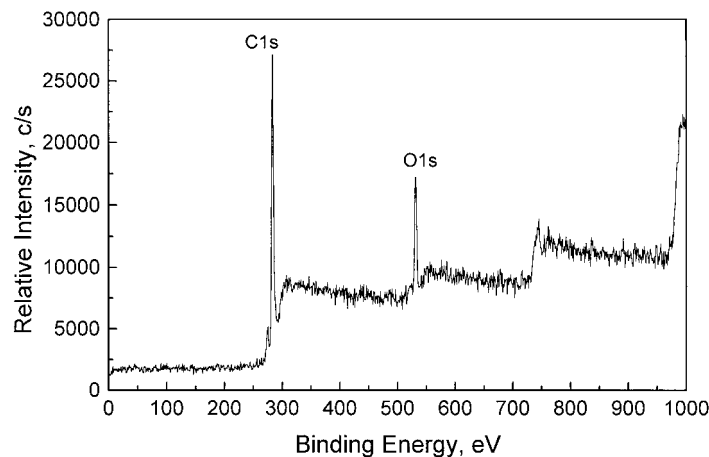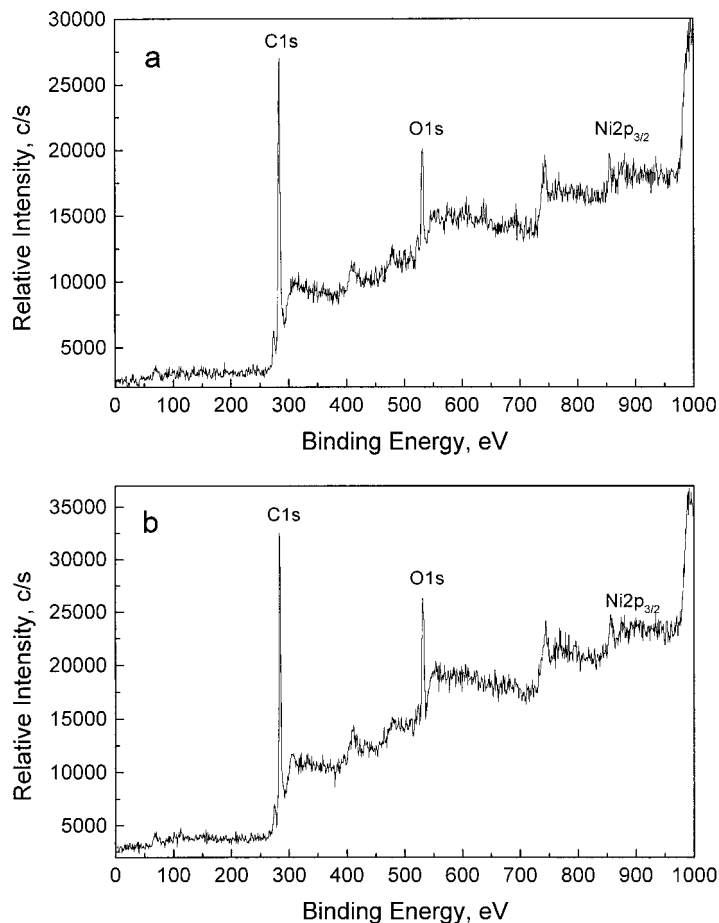

Figure 4 ESCA spectra of B.

Figure 5   ESCA spectra of (a) B-1 and (b) B-11.

a 20-nm diameter. The grayish white parts correspond to PHEMA as the shell of the particles with a 10-nm thickness [Fig. 1(c)].

Characterization of PSt-*b*-PHEMA Metal Hybrids

The polymer-supported metal composites, PSt-*b*-PHEMA/Ni (B-11), PSt-*b*-PHEMA/Co (B-22), and PSt-*b*-PHEMA/Ni—Co (B-33) were prepared by reducing the corresponding block copolymer/metal ionic complexes, B-1, B-2, and B-3. Figure 2 shows the morphologies of B-1, B-11, B-2, B-22, B-3, and B-33. Compared with Figure 1(b,c), we can see that for the polymer–Ni^{2+} complex uniform spherical particles were not formed, and in the case of the polymer–Co^{2+} complex, polydisperse spherical particles were produced, indicating that the metal ions greatly affect the phase-separation process. As the DMF and water in the PSt-*b*-PHEMA solution evaporated, microphase separation occurred gradually, the PSt block aggregated to form a spherical core, and PHEMA surrounded the core as show in Figure 1(b,c).

When metal ions are added into this polymer solution, the complexing of the metal ion with PHEMA prevents the PHEMA segment to aggregate around the core. So, in the polymer and metal-ion system, there are two competition factors affecting the morphology of the polymer and metal-ion film during separation: The higher binding energy of Ni^{2+} and oxygen favors the aggregation of the PHEMA segment, and it competes with the aggregation of PSt, resulting a short stripe texture as shown in Figure 2(a). The lower binding energy of Co^{2+} and oxygen does not compete with the aggregation of the PSt segment, so bigger spherical particles were formed as shown in Figure 2(c). For Co^{2+}, Ni^{2+}, and the polymer system, we can imagine that the Ni^{2+} ion promotes the aggregation of the PHEMA segments. Figure 2(e) is the result of that these spherical particles are connected to each other.

Figure 3 shows the XRD profiles of B, B-1, B-11, B-3, and B-33. In addition to the diffraction peaks of B, some additional peaks occurred in the
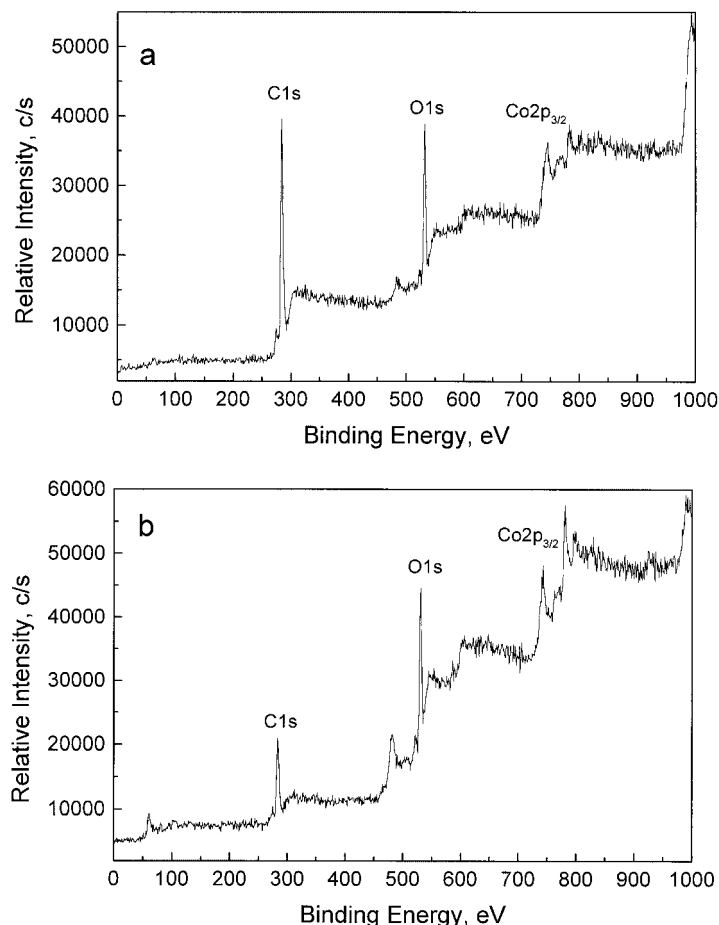
Figure 6   ESCA spectra of (a) B-2 and (b) B-22.

patterns of B-1, B-11, B-3, and B-33. There were no new peaks obtained in B-2 and B-22, because the absorption of cobalt using CuKα is very great; thus, the cobalt peak is not observed. Based on the data listed in the *Powder Diffraction File*,[16] the new phase in B-1 is hexagonal nickel hydroxide and that in B-11 is nickel. Although we cannot exactly identify the existence of cobalt directly from the peak value in Figure 3(d,e), in comparison of the *d* value of B-3 and B-33 with the data listed in the *Powder Diffraction File*, the values of *d* in Figure 3(d,e) were, respectively, larger than those of nickel hydroxide or nickel and smaller than those of cobalt hydroxide and cobalt. Thus, we deduced that the phase in B-3 belongs to the mixture of hexagonal nickel and cobalt hydroxides, and the new phase in B-33 is the mixture of nickel and cobalt. As we know, the values of the *a* and *c* axes of hexagonal nickel hydroxide are correspondingly smaller than are those of hexagonal cobalt hydroxide. In comparing Figure 3(c) with Figure 3(e), the peak in Figure 3(e) became wide,

illustrating the existence of the cobalt and nickel alloy in B-33.

ESCA analysis showed the binding energies for the B, B-1, B-11, B-2, B-22, B-3, and B-33 samples (Figs. 4–7), and the values of the binding energy are listed in Table II. Compared with the value of $Ni2P_{3/2} = 855.9$ eV in the *Handbook of X-ray Photoelectron Spectroscopy*,[17] the nickel existed as nickel hydroxide[17] in B-1 and B-3 and the cobalt existed as cobalt hydroxide ($Co2P_{3/2} = 780.5$ eV)[17] in B-2 and B-3. These results are according to the results of the XRD. The nickel exists as nickel oxide ($Ni2P_{3/2} = 854.8$ eV)[17] in B-11 and B-33 and the cobalt exists as cobalt oxide ($Co2P_{3/2} = 780$ eV) in B-22 and B-33. These results do not coincide with the results of the XRD. Because ESCA examines the metal state on the surface, after the polymer metal-ion complexes were reduced using KBH_4, the nanometer metal particles [Ni(0) or Co(0)] on the surface were formed and oxidized easily in air to form
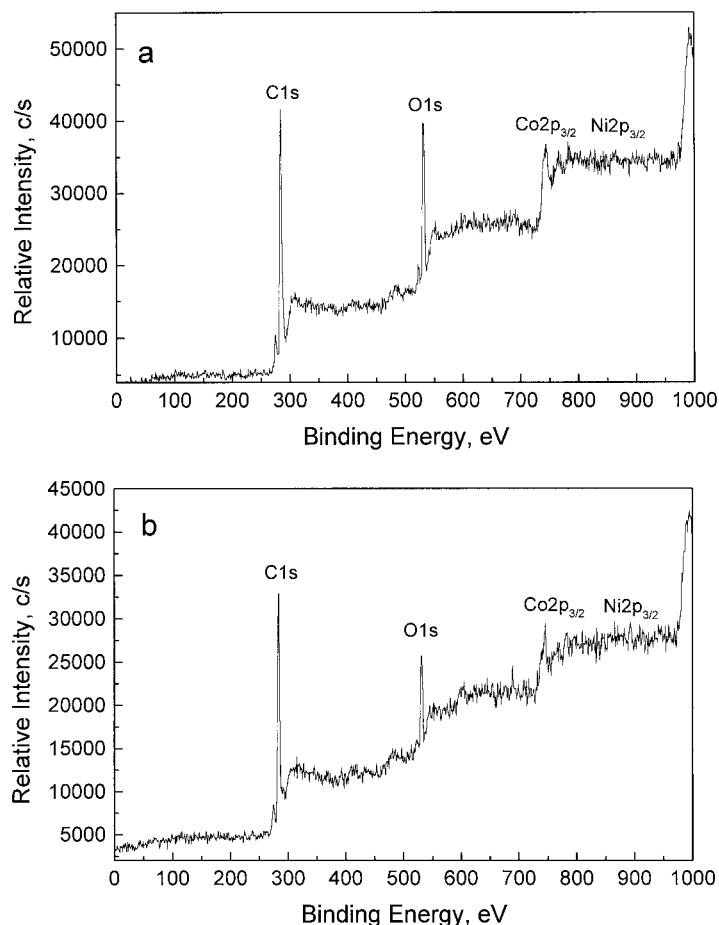
Figure 7 ESCA spectra of (a) B-3 and (b) B-33.

NiO or CoO. The same phenomenon was observed.[18,19]

The data listed in Table II show that the contents of metal ions measured by ESCA are generally lower than are those obtained by the AAS method, which means that the metal ions on the surface of the composite particles are fewer than are those in the inner polymer–metal composites. When considering the formation process of the composites, it is easier to understand. As we discussed, a stronger complex ability of Ni^{2+} with PHEMA connects PHEMA segments to form film

Table II   Metal Content of Polymer Metal Hybrids

Sample[a]	Ni (%)[b] AAS	Co (%)[b] AAS	Ni (%)[c] ESCA	Co (%)[c] ESCA	Ni2P$_{3/2}$ Binding Energy (eV)	Co2P$_{3/2}$ Binding Energy (eV)
B-1 (B–Ni^{2+})	8.12		1.40		856.40	
B-11 (B–Ni)	8.19		2.09		854.20	
B-2 (B–Co^{2+})		7.97		2.06		781.00
B-22 (B–Co)		7.64		3.45		779.80
B-3 (B–Ni^{2+}/Co^{2+})	3.55	5.96	0.65	1.48	856.50	781.20
B-33 (B–Ni/Co)	3.26	5.92	1.63	1.74	853.90	779.00

[a] Block copolymer B in Table I was used.
[b] Measured by atomic absorption spectrum.
[c] Measured by electron spectroscopy chemical analysis.

as shown in Figure 2(a). For the Co^{2+} composites, bigger spherical particles were formed due to a lower complex ability of Co^{2+} with PHEMA. In addition, when putting the polymer–metal ion solution into water, for washing ammonia, the free hydroxyl group of PHEMA will locate on the surface of the particles during the microphase separation. So, the surface area of the composites contains fewer metal ions. In comparison with the Ni^{2+} composite, a lower binding energy of Co^{2+} with oxygen favors the diffusion of Co^{2+} in the inner composite to the surface; thus, a higher content of Co^{2+} on the surface area than that of Ni^{2+} was observed (see Table II). When the dispersions of the metal-ion–polymer composites in water were reduced by KBH_4, the reduction occurred on the surface at first, the metal (0) will aggregate to form nanoparticles as shown in Figure 2(b,d,f), and then some metal ions in the inner part of the composites will diffuse to the surface. Therefore, the metal (0) contents on the surface (see B-11, B-22, and B-33) are higher than are those of the corresponding metal-ion composites (see B-1, B-2, and B-3).

CONCLUSIONS

A narrow polydispersity block copolymer PSt-*b*-PHEMA was prepared by the ATRP method. Core–shell particles were formed due to microphase separation as DMF and water gradually evaporated. The addition of Co^{2+} and Ni^{2+} ions into the PSt-*co*-PHEMA solution in DMF and water will greatly affect the microphase-separation process and, lastly, the morphologies of the metal-ion–polymer composite. There is an equilibrium between the aggregation on PSt and the metal ion complexing with PHEMA. The former forms spherical particles; the latter favors the formation of a stripe in the composite film. The stronger binding energy of $N1^{2+}$–oxygen favors the aggregation of PHEMA segments to form a short striped texture in the film. The lower binding energy of Co^{2+}–oxygen affords bigger spherical particles. In comparison of the metal ion composites, the metal contents on the surface are greater than are those of the corresponding metal-ion composites, because the reduction occurs on the surface at first and then the metal ions in the inner composites diffuse to the surface.

REFERENCES

1. Saito, R.; Okamura, S.; Ishizu, K. Polymer 1996, 37, 5255–5259.
2. Moffitt, M.; Eisenberg, A. Chem Mater 1995, 7, 1178.
3. Moffitt, M.; Mcmahon, L.; Pessel, V.; Eisenberg, A. Chem Mater 1995, 7, 1185.
4. Antonietti, M.; Wenz, E.; Bronstein, L.; Seregina, M. Adv Mater 1995, 7, 1000.
5. Cheang Chan; Ng, Y.; Schrock, R. R.; Cohen, R. E. Chem Mater 1992, 4, 24.
6. Cheang Chan, Ng, Y.; Schrock, R. R.; Cohen, R. E. J Am Chem Soc 1992, 114, 7295.
7. Cummins, C. C.; Ng, Y.; Schrock, R. R.; Cohen, R. E. Chem Mater 1992, 4, 27.
8. Saito, H.; Okamura, S.; Ishizu, K. Polymer 1992, 33, 1099.
9. Saito, R.; Okamura, S.; Ishizu, K. Polymer 1993, 34, 1189.
10. Saito, R.; Okamura, S.; Ishizu, K. Polymer 1993, 34, 1183.
11. Antonietti, M.; Forster, S.; Hartmann, J.; Oestreich, S. Macromolecules, 1996, 29, 3800.
12. Wenz, E.; Thunemann, A.; Antonietti, M. Colloid Polym Sci 1996, 274, 795.
13. Wang, J. S.; Matyjaszewsk, K. J Am Chem Soc 1995, 117, 5614.
14. Wang, J. S.; Matyjaszewsk, K. Macromolecules 1995, 28, 7901.
15. Gaynor, S. G.; Edelman, S. Z.; Matyjaszewski, K. Macromolecules 1996, 29, 1079.
16. Joint Committee on Powder Diffraction Standards, Inorganic Index to the Powder Diffraction File; The Joint Committee on Diffraction Standards: Swarthmore, PA, 1972.
17. Wager, C. D.; Riggs, W. M.; Davis, L. Z.; Moulder, J. F.; Muilenberg, G. E. Handbook of X-ray Photoelectron Spectroscopy; Perkin–Elmer's Physical Electronics Division: Eden Prairie, MN, 1979.
18. Tamai, H.; Sakurai, H.; Hirota, Y.; Nishiyama, F.; Yasuda, H. J Appl Polym Sci 1995, 56, 441.
19. Wang, Y. M.; Feng, L. X.; Pan, C. Y. J Appl Polym Sci 1998, 70, 2307.